

Optimal control based seizure abatement using patient derived connectivity

Peter Neal Taylor, Jijju Thomas, Nishant Sinha, Justin Dauwels, Marcus Kaiser, Thomas Thesen and Justin Ruths

Journal Name:	Frontiers in Neuroscience
ISSN:	1662-453X
Article type:	Methods Article
First received on:	03 Apr 2015
Revised on:	14 May 2015
Frontiers website link:	www.frontiersin.org

Optimal control based seizure abatement using patient derived connectivity

Peter Neal Taylor^{1,*}, Jijju Thomas², Nishant Sinha³, Justin Dauwels³, Marcus Kaiser^{1,4}, Thomas Thesen⁵ and Justin Ruths²

¹*Interdisciplinary Computing and Complex BioSystems (ICOS) Research Group, School of Computing Science, Newcastle University, Newcastle upon Tyne, UK*

²*Engineering Systems and Design, Singapore University of Technology and Design, Singapore*

³*School of Electrical and Electronic Engineering, Nanyang Technological University, Singapore*

⁴*Institute of Neuroscience, Newcastle University, Newcastle upon Tyne, UK*

⁵*Department of Neurology, New York University, New York, USA*

Correspondence*:

Corresponding Author

School of Computing Science, Newcastle University, Newcastle upon Tyne, NE1 7RU, UK, peter.taylor@ncl.ac.uk

2 ABSTRACT

3 Epilepsy is a neurological disorder in which patients have recurrent seizures. Seizures
4 occur in conjunction with abnormal electrical brain activity which can be recorded by the
5 electroencephalogram (EEG). Often, this abnormal brain activity consists of high amplitude
6 regular spike-wave oscillations as opposed to low amplitude irregular oscillations in the non-
7 seizure state. Active brain stimulation has been proposed as a method to terminate seizures
8 prematurely, however, a general and widely-applicable approach to optimal stimulation protocols
9 is still lacking.

10 In this study we use a computational model of epileptic spike-wave dynamics to evaluate the
11 effectiveness of a pseudospectral method to simulated seizure abatement. We incorporate brain
12 connectivity derived from magnetic resonance imaging of a subject with idiopathic generalized
13 epilepsy.

14 We find that the pseudospectral method can successfully generate time-varying stimuli that
15 abate simulated seizures, even when including heterogeneous patient specific brain connectivity.
16 The strength of the stimulus required varies in different brain areas.

17 Our results suggest that seizure abatement, modeled as an optimal control problem and solved
18 with the pseudospectral method, offers an attractive approach to treatment for *in vivo* stimulation
19 techniques. Further, if optimal brain stimulation protocols are to be experimentally successful,
20 then the heterogeneity of cortical connectivity should be accounted for in the development of
21 those protocols and thus more spatially localized solutions may be preferable.

22 **Keywords:** Optimal Control; Numerical Methods; Epilepsy model; Connectome; Bistability; Spike-wave; Stimulation

1 INTRODUCTION

23 Epilepsy is a spectrum of disorders in which patients have seizures due to abnormal neuronal activity
24 (**Blumenfeld and Taylor, 2003**). Symptomatic manifestations of these events can include a loss
25 of consciousness, tonic-clonic convulsions and myoclonic jerks, amongst others which can severely
26 impact patient quality of life. These transient seizure events often have distinctive electrographic
27 correlates detectable on the electroencephalogram (EEG). One commonly observed electrographic seizure
28 manifestation is the spike wave discharge (SWD). SWDs are high amplitude periodic oscillations with
29 a frequency typically slower than that of normal awake EEG. They are often associated with absence
30 seizures, myoclonic seizures and complex partial seizures (**Asconapé and Penry, 1984; Sadleir et al.,**
31 **2006**). Currently the first line of treatment for patients with epilepsy is typically medication, however in
32 over 30% of cases medication alone is insufficient (**Keränen et al., 1988**).

33 Brain stimulation has been suggested as an alternative therapeutic treatment for epilepsy (**Liang et al.,**
34 **2010, 2012; Sallet et al., 2012; Berényi et al., 2012**). In addition, it has also been suggested that
35 noninvasive stimuli such as an auditory tone (**Rajna and Lona, 1989**) or through the use of transcranial
36 magnetic stimulation (TMS) (**Conte et al., 2007**) could be used to interrupt SWD seizures in humans.
37 Unfortunately optimal parameters for stimulation for the abatement of SWD seizures are currently
38 unknown. Attempting to elucidate optimal control parameters in an experimental / clinical setup is difficult
39 due to various ethical, safety and financial reasons.

40 *In silico* testing of stimulation protocols offers a complementary approach to *in vivo* experimentation.
41 Indeed, several computational models of epileptiform SWD exist at the macroscopic spatial scale which
42 is routinely recorded clinically using EEG. However, many of these models treat the cortex as a spatially
43 continuous homogeneous medium (**Breakspear et al., 2006; Robinson et al., 2002; Marten et al., 2009**),
44 or disregard spatial interactions altogether (**Wang et al., 2012**). In contrast, it has been suggested that
45 spatial heterogeneities may be important in seizure genesis or maintenance (**Kramer and Cash, 2012;**
46 **Terry et al., 2012; Westmijse et al., 2009**) and should therefore be incorporated into a model (**Baier**
47 **et al., 2012**).

48 Recent years have seen the development of brain imaging protocols using magnetic resonance imaging
49 (MRI) which enable the inference of heterogeneous subject-specific brain connectivity. It is essentially
50 possible to generate a connectivity matrix representing the brain network, with brain areas represented
51 by nodes, and edges / connections inferred using tractography algorithms passing through the white
52 matter. The so-called structural connectome (**Sporns et al., 2005**), represented as a matrix, can be directly
53 incorporated into a computational model of brain activity. Several previous studies have used this approach
54 to simulate healthy brain function (**Honey et al., 2009; Deco et al., 2013; Haimovici et al., 2013; Messé**
55 **et al., 2014**). However, very few have simulated epileptic activity (**Taylor et al., 2014a, 2013b; Yan and**
56 **Li, 2013**).

57 The control of a system with SWD oscillations is highly nontrivial since the system is nonlinear (**Taylor**
58 **et al., 2014b**). The goal of seizure abatement through stimulation can be cast as an optimal control
59 problem, which provides a systematic and general approach for designing stimuli. Control theory's
60 traditional analytical techniques, however, do not scale well as the size of the system increases, as is the
61 case in considering a model with spatial heterogeneities. In recent years the pseudospectral method has
62 been applied successfully in a variety of applications as a highly efficient, robust method for the control
63 of large-scale nonlinear systems (**Ruths and Li, 2012**). In this study we use the pseudospectral method
64 to design time-varying stimuli for SWD seizure abatement *in silico* cast as optimal control problems. The
65 open-loop controls developed by this technique offer distinct advantages in terms of being less invasive
66 and more robust over alternative methods that employ feedback. We test the robustness of our method by
67 applying the approach in different settings. We begin with a relatively simple model which neglects spatial
68 interactions and ultimately build up to large-scale control of a stochastic model using connectivity derived
69 from a patient with clinically diagnosed idiopathic generalized epilepsy. To our knowledge this is the first
70 epilepsy modeling study using patient derived diffusion MRI based connectivity and consequently also
71 the first attempt to control seizures in such a model.

2 MATERIAL & METHODS

2.1 IMAGING

72 Cortical connectivity was inferred from a 22 year old female patient clinically diagnosed with idiopathic
 73 generalized epilepsy with a history of absence and generalized tonic clonic seizures. The subject gave
 74 their written informed consent to participate in this study, which was approved by the Institutional Review
 75 Board of NYU Langone School of Medicine. T1 structural MRI and DTI images were acquired using a
 76 Siemens Allegra 3T scanner. Diffusion images were collected using 64 directions, with a b -factor of 1000 s
 77 mm^{-2} , one b_0 image and 2.5mm isovoxel, TR=5500ms, TE=86ms. A T1 anatomical image also acquired
 78 using the following parameters: TR=2530ms, TE=3.25ms, FOV=256mm at a resolution of 1x1x1.33mm.

79 To infer the cortico-cortical connectivity of the patient we first, using the T1 image, segmented white
 80 matter and grey matter areas, then performed parcellation of the grey matter into 66 regions of interest.
 81 These regions of interest correspond to major gyral-based anatomical areas which have been shown to
 82 be highly consistent between subjects (Desikan et al., 2006). These grey matter volume ROIs generated
 83 using FreeSurfer (<http://surfer.nmr.mgh.harvard.edu>) were then imported into DSI studio
 84 (Yeh et al., 2010) along with the motion corrected diffusion images. Whole brain seeding was then used
 85 and tractography was performed. Only tracts with both ends terminating in the grey matter were retained.
 86 When a total of 5,000,000 tracts were found tractography was terminated. With the tracts and the ROIs
 87 registered to the same space the mean fractional anisotropy along tracts connecting two ROIs was then
 88 taken as a connectivity weight. This weighted structural connectivity matrix (M) is then used in the model
 89 to directly represent cortical connectivity of the patient. Figure 1 summarizes the image processing. A full
 90 list of ROI names can be found in table S1.

2.2 MODEL

91 **2.2.1 Spatially independent** Experimental evidence suggests important roles for both the cortex and
 92 thalamus in the genesis and maintenance of epileptic SWD oscillations (Destexhe, 1998; Pinault and
 93 O'Brien, 2005). We therefore incorporate knowledge of these anatomical structures into our model using
 94 neural field equations based on the Amari framework (Amari, 1977) which has been previously used
 95 to model SWD (Taylor and Baier, 2011; Taylor et al., 2014b). The cortical subsystem is composed of
 96 excitatory pyramidal (PY) and inhibitory interneuron (IN) populations. The thalamic subsystem includes
 97 variables representing populations of thalamocortical relay cells (TC) and neurons located in the reticular
 98 nucleus (RE). All populations are interconnected in agreement with experimentally known connections
 99 (Pinault and O'Brien, 2005) using the connectivity parameters $C_{1...9}$. The resulting model equations are
 100 therefore:

$$\begin{aligned}
 \dot{PY}(t) &= \tau_1 (h_{py} - PY + C_1 f[PY] & (1) \\
 &\quad - C_3 f[IN] + C_9 f[TC]) + u(t) \\
 \dot{IN}(t) &= \tau_2 (h_{in} - IN + C_2 f[PY]) + u(t) \\
 \dot{TC}(t) &= \tau_3 (h_{tc} - TC - C_6 s[RE] \\
 &\quad + C_7 f[PY]) \\
 \dot{RE}(t) &= \tau_4 (h_{re} - RE - C_4 s[RE] \\
 &\quad + C_5 s[TC] + C_8 f[PY])
 \end{aligned}$$

where $h_{py,in,tc}$ are input parameters, $\tau_{1...4}$ are timescale parameters and $f[x]$ is the sigmoid function :

$$f[x] = (1/(1 + e^{-x})) \quad (2)$$

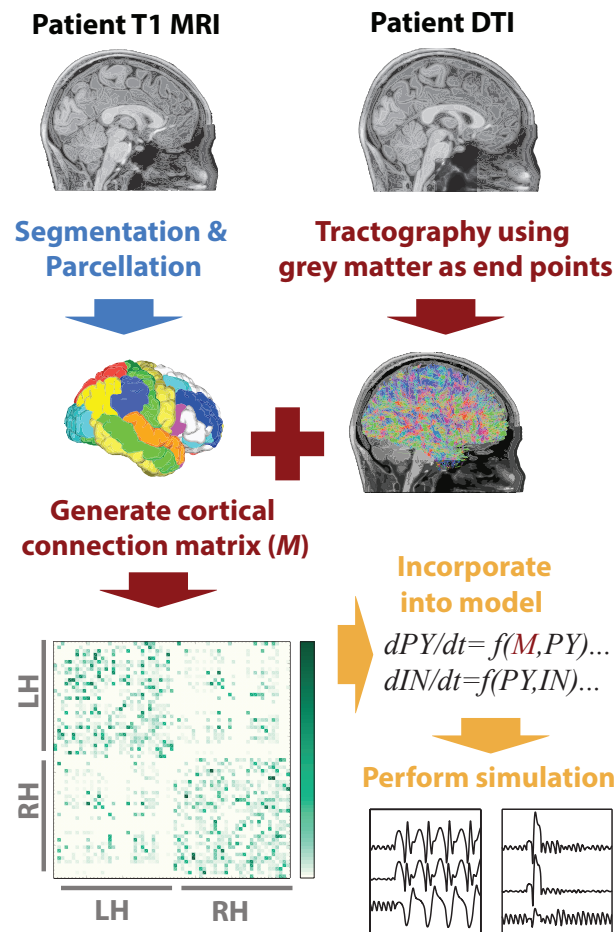


Figure 1. MRI processing and modelling pipeline. A patient-specific connectivity matrix is generated using anatomical T1 and diffusion weighted MRI. Segmentation and parcellation are performed using FreeSurfer (blue arrow) to define network nodes and tractography is performed using DSI Studio (red arrows) to determine connections in the network. Custom Matlab code is used to import the connectivity and simulate the model (orange arrows).

101 in which $x = PY, IN, TC, RE$ and ϵ determines the sigmoid steepness. We simplify the thalamic
 102 subsystem by using a linear activation term $s[x] = ax + b$ instead of the sigmoid function $f[x]$ since
 103 this does not qualitatively impact the dynamics and makes analysis simpler (Taylor et al., 2014b). This
 104 follows the connection schematic as shown in figure S1 based on (Pinault and O'Brien, 2005).

105 Deterministic model solutions of equation 1 are simulated numerically using ode45 in MATLAB.
 106 Stochastic model solutions are computed numerically using a fixed step Euler-Maruyama solver in
 107 MATLAB with a step size (h) of 1/15000 seconds. Equations for the noise driven system are given in
 108 supplementary methods section 1. Stimulations to induce SWD are simulated as a perturbation to the PY
 109 and IN variables in state space where the control (stimulus) $u(t)$ is applied to the cortical variables only.
 110 Parameters are identical to those used in Taylor et al. (2014b).

111 **2.2.2 Spatially extended** Following simulations with only one cortical area, the model can easily
 112 be extended to include multiple cortical areas. In our model the cortical areas have local connectivity
 113 within an area through reciprocal $PY \rightarrow IN$ and $IN \rightarrow PY$ connections in addition to long range excitatory
 114 connections only. Long range connections (on the order of several centimeters in length) have been shown
 115 experimentally to be predominantly excitatory. We therefore incorporate this into our model using the

116 patient-specific DTI matrix M to represent $PY \leftrightarrow PY$ connections. This approach of incorporating long
117 range connectivity as excitatory is in agreement with previous modeling studies (**Babajani-Feremi and**
118 **Soltanian-Zadeh**, 2010) and follows the connectivity schematic and equation in supplementary methods
119 part 2.

2.3 OPTIMAL CONTROL

120 Broadly speaking, optimal control is a mathematical framework for systematically selecting the time-
121 varying input needed to drive a dynamical system in a desired way. In general, many choices of input,
122 or stimuli, might achieve a desired objective and without the formalism of optimal control selecting
123 one of these options from a family of potential stimuli is ad-hoc and ill-defined. An optimal control
124 problem couples a cost, or fitness, function to be minimized (or potentially maximized) with a set of
125 constraints. Setting it apart from conventional optimization problems is that this set of constraints includes
126 the differential (or difference) equation that captures the dynamics of the system (**Luenberger**, 1968).
127 Initial (at the start time, $t = 0$) conditions and often final (at the final time, $t = T$) constraints also exist.
128 Path constraints that are imposed over the entire time window $t \in [0, T]$ are also possible. Most critically,
129 the cost function must be selected appropriately to evaluate the candidate options of stimuli and select the
130 correct one.

131 While the framework of optimal control can capture such a desired objective well, the techniques to
132 solve optimal control problems analytically are limited, especially for large-scale and nonlinear systems.
133 We, therefore, turn to computational methods to solve them. The pseudospectral method is an ideal
134 computational method for this purpose, namely for practitioners in a variety of applied disciplines to
135 use, due to its high level of accuracy and ease of implementation.

136 The method benefits, like other spectral methods (e.g., Fourier series), from the exponential
137 convergence, as the order of approximation increases, characteristic of orthogonal functions (**Fornberg**,
138 1998). In this case we use the Legendre polynomials to approximate the states and control. The method
139 also relies (the “pseudo” part of the name) on a recursive relation between the Lagrange interpolating
140 polynomials and the Legendre polynomials, so that the approximation can be instead approximated by
141 Lagrange polynomials, leading to a double approximation: the unknown states/controls to the Legendre
142 approximation to the Lagrange approximation (**Canuto et al.**, 2006). As the second approximation is
143 an interpolation, the coefficients of the Lagrange approximation are the values of the states and controls
144 themselves at the discretized time points, rather than more abstract coefficients of the Legendre expansion.
145 The latter case (where abstract coefficients are used) is what occurs in a Fourier series approximation of
146 a signal. The coefficients have an interpretation, but the information gleaned is indirect information about
147 the signal itself. These two factors, the *pseudo* and *spectral*, make the method both easy to implement,
148 efficient, and, when combined with standard nonlinear optimization solvers, a powerful and scalable
149 approach for solving optimal control problems.

150 Ultimately, the pseudospectral method utilizes these approximations to discretize (in time) the
151 continuous optimal control problem into a nonlinear optimization problem. The decision variables of the
152 subsequent optimization problem are the coefficients of the Lagrange interpolating polynomial, which are
153 also the values of the unknown state and control functions at the discretization points. This optimization
154 problem can be solved using any number of commercial or open-source nonlinear solvers. While nonlinear
155 optimization is still a field of much research, the work to-date has produced a number efficient algorithms
156 that scale well on large-scale problems. In order to recover the state and control functions from the
157 discretized solution, we construct the Lagrange approximating polynomial from the optimal decision
158 variables.

159 A complete presentation of the pseudospectral method and implementation can be found in the
160 supplementary text.

161 In this work, we use a cost that minimizes the input power (the integrated square of the input). Such a
162 cost function both reduces the invasiveness of the stimuli and also tends to produce inputs that are more

163 interpretable, as they are devoid of non-essential fluctuations in the control shape. We also impose state
164 constraints at the initial and final time to enforce the desired state transfer. Finally, time is discretized into
165 81 nodes (using a Lagrange approximation of 81 terms), which is dramatically smaller when compared
166 with other methods, such as Runge-Kutta.

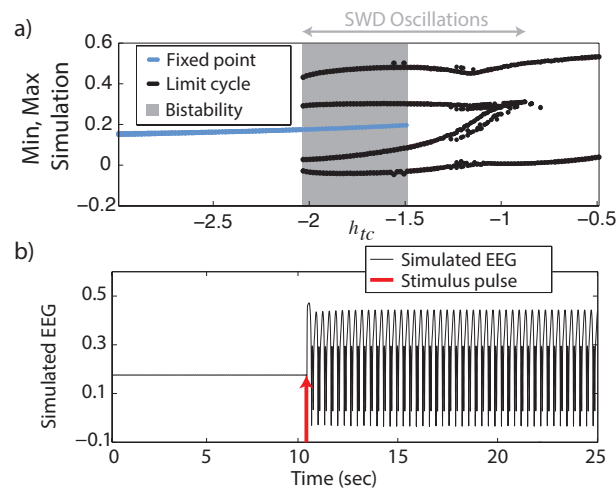


Figure 2. Bifurcation diagram. a) Minima and maxima of time series for different values of h_{tc} . A fold of cycles bifurcation occurs at the transition between bistability and excitability. b) Time series of the model output

3 RESULTS

3.1 MODEL DYNAMICS

167 We begin with the simplest of our scenarios. We investigate the model without noise (i.e. purely
 168 deterministic) and independent of any lateral spatial interactions (equation 1). Figure 2a shows the maxima
 169 and minima of the model output for different values of the parameter h_{tc} . For more negative values shown
 170 ($h_{tc} < \approx -2$, left side of figure) there is only one stable solution, all simulations converge to the steady
 171 state (stable focus). For less negative values ($-2 < \approx h_{tc} < -1.5$, shaded area of figure) a bistable region
 172 exists between the stable focus and the SWD oscillations. This arises following a fold of cycles bifurcation
 173 at $h_{tc} \approx -2$. Beyond the disappearance of the stable focus (due to a subcritical Hopf bifurcation) at
 174 $h_{tc} > -1.5$, monostable SWD and slow waves exist (right hand side of figure). In the bistable region
 175 a separating manifold (separatrix) exists between the two states in four dimensional state space. This
 176 manifold is highly complex in structure (Taylor et al., 2014b).

177 The stable focus can be considered analogous to resting state background EEG, and the high amplitude
 178 oscillatory attractor to be the seizure state (Kalitzin et al., 2010; Taylor et al., 2014b). Transitions
 179 between non-seizure and seizure states can occur when a stimulus beyond the separatrix occurs. When
 180 this does occur in the bistable region a further stimulus is required to stop the SWD, if a second stimulus is
 181 not given the SWD will continue indefinitely. In figure 2b we show an example time series following such
 182 a stimulus. In the region immediately preceding the bifurcation at $h_{tc} \approx -2$ complex excitable transients
 183 occur lasting several seconds (figure S3a). Ultimately the goal of stimulus driven seizure abatement is to
 184 minimise the duration of the seizure following detection.

3.2 OPTIMAL CONTROL OF DETERMINISTIC SPIKE-WAVE DYNAMICS

185 The control of SWD implemented here requires a two-step process; seizure detection and seizure control.
 186 The seizure is detected when the PY and IN variables are in the proximity of a point specified on the
 187 bistable limit cycle. This could easily be adapted in an experimental setting by using delay embedding
 188 to predict state variables (Taylor et al., 2014b; Babloyantz and Destexhe, 1986; Takens, 1981). Since
 189 the SWD is fairly regular between cycles and between seizures this ‘trigger point’ can be used, provided
 190 that the seizure activity passes close by in state space (e.g., within an error tolerance of $\pm 10\%$). In theory
 191 all points on the SWD limit cycle could be used as trigger points to decrease the time taken to detect and

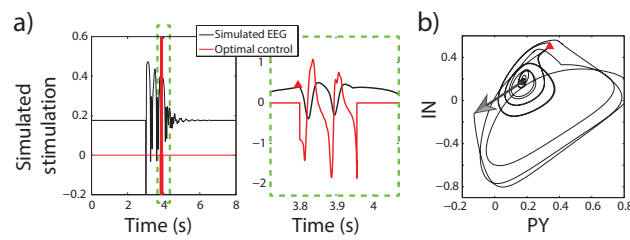


Figure 3. Control of bistable SWD Time series of model and control in the bistable parameter setting (as used in figure 2). Projection of the PY and IN variables in phase space are shown in b). Red triangle indicates the trigger point at which the control was applied. The large arrow indicates the stimulus to induce the SWD.

192 subsequently control the seizure, where each point would correspond to a stimulus with a different profile.
 193 This would mean that the stimulus could be applied at any phase in the spike. However, we limit ourselves
 194 in this study to a single arbitrarily chosen point and leave optimal seizure *detection* for future study.

195 Once the SWD has passed close enough to the trigger point the seizure is detected and the control
 196 stimulus is applied starting at that time instant. Figure 3b shows the state space for the PY and IN
 197 variables. A stimulus to initiate a seizure is indicated by an arrow, while the red \triangle indicates the trigger point. In
 198 both the bistable and excitable cases the seizure is abated prematurely by the control (red lines in figures
 199 3a). An important advantage of the control applied here is that the same control is applied to both the
 200 PY and IN variables, while the TC and RE variables are not controlled. This would be desirable in the
 201 experimental scenario where a stimulus may activate multiple neuron types with the same waveform
 202 morphology and is nonselective. Likewise, stimuli for the TC and RE variables could be developed using
 203 the same framework.

204 Figure 3 shows successful SWD abatement when the model is placed in the bistable setting. Interestingly
 205 the same profile can also be used in the excitable transient parameter setting since the flows in state space
 206 are similar (figure S3).

3.3 OPTIMAL CONTROL OF STOCHASTIC SPIKE-WAVE DYNAMICS

207 The simulated seizures shown in figure 3 are artificial in the sense that they are induced by a stimulus at 3
 208 seconds, indicated by the arrow in state space. In figure 4 we test the capability of the control stimulus to
 209 abate a spontaneously occurring simulated seizure with the inclusion of noise. This has proven extremely
 210 challenging in a previous study where noise has been shown to impact the success rate significantly
 211 (Taylor et al., 2014b). For comparison, the upper panel of figure 4 shows a clinical recording of one
 212 EEG channel from a patient exhibiting transitions between non-seizure and seizure states. This compares
 213 favorably with the stochastic model simulation (figure 4b). Irregular oscillations around the stable focus
 214 driven by noise resemble background activity with an abrupt onset of SWD. Figure 4b shows a simulation
 215 without any external control. In figure 4c, the same control signal in figure 3 is applied.

216 The challenge with dealing with stochasticity and the success here with this method underscores the
 217 importance of a systematic approach to seizure abatement. Because the optimal control drives the system
 218 from near a known trigger point in state space to the background state, the effects of stochasticity are
 219 minor. Ad-hoc approaches that work in the deterministic case, may be highly sensitive to the perturbations
 220 introduced when noise is added. In previous work (Ruths et al., 2014), we demonstrate how ensemble
 221 control can be used to develop stimuli that are robust to variation in the initial state. This situation arises
 222 when the noise driven process and the delays in triggering cause the state to shift noticeably before the
 223 control can be applied. Because of the consistency of the bistable model, the excitable case requires this
 224 extra step of making the stimulus more robust.

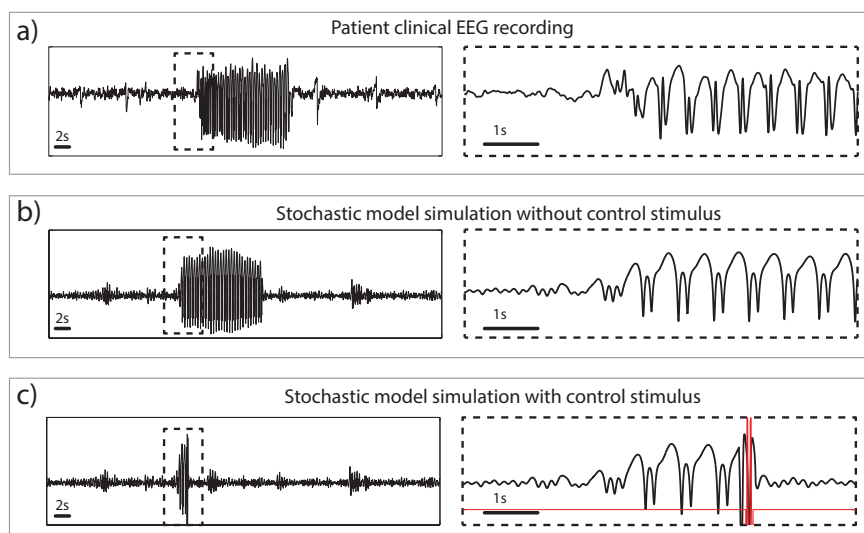


Figure 4. Clinical and simulated stochastic time series with and without control. a) Patient recording from a scalp electrode during a seizure. b) Stochastic model simulation without control. c) Stochastic model simulation with control turned on.

3.4 OPTIMAL CONTROL OF HETEROGENEOUS SPIKE-WAVE DYNAMICS

225 We now apply our method to a case which incorporates patient-derived brain connectivity data. Despite
 226 idiopathic generalized epilepsy involving widespread bilateral brain areas, it has been argued that
 227 heterogeneity in brain connectivity may contribute to seizure genesis and maintenance (Taylor et al.,
 228 2013a). Indeed, it has been suggested that an improved understanding of the heterogeneities involved may
 229 lead to more effective treatments for spike-wave seizures (Blumenfeld, 2005). We therefore incorporate
 230 patient-specific heterogeneous brain connectivity into our model.

231 For comparison we include a clinical recording of a generalized SWD seizure in figure 5a. Figure 5b
 232 shows a simulation of the model which incorporates the patient based structural connectivity. The model
 233 is capable of reproducing various features seen clinically, specifically with respect to spatial variation
 234 between recording electrodes. Three simulated channels are zoomed to enable closer examination. They
 235 show high, and low amplitude spikes (first two panels) in addition to slow wave oscillations, all of these
 236 features are routinely observed clinically (for examples see e.g. Baier et al. (2012) and panel a) in figure
 237 5).

238 To abate the simulated seizure we apply our optimal control method to all simulated cortical brain areas.
 239 Figure 5c shows a time series of a simulated seizure with the control enabled. With the exception of the
 240 controls being applied, the model parameters and noise are identical to that shown in figure 5b. With
 241 the control stimuli applied the simulated seizure is terminated almost immediately in all channels. This
 242 is despite the spatial heterogeneity in waveform morphology across channels and stimuli. The control
 243 signals are shown for three of the simulated brain areas in red in figure 5c. There are some noticeable
 244 differences in morphology and amplitude between the channels. For example, the bottom of the three
 245 panels has a much larger positive deflection compared to the other two at the start, while at the end the
 246 negative deflection is much weaker. Due to the underlying heterogeneity some brain areas require more
 247 total energy to abate (absolute sum of power over time). In essence the total control needs to be stronger
 248 for some brain areas than others. Figure 5d shows the strength of stimulus applied for optimal control
 249 in different brain areas. Superior frontal areas (more red areas) require more power than occipital areas
 250 (more white in color).

4 DISCUSSION

251 In this study we have applied optimal control to a model of epileptiform SWD oscillations incorporating
252 patient-derived connectivity to prematurely abate the simulated seizure. To our knowledge this is the first
253 study to incorporate diffusion MRI based connectivity from a patient into a macroscopic model of epilepsy
254 and also the first attempt at simulating control using a human derived DTI network. We showed that the
255 control can work in different settings (excitable / bistable, stochastic / deterministic) and with different
256 spatial properties (space-independent, heterogeneously spatially-extended).

257 Previous modeling attempts of seizure control have included several different approaches. One approach
258 is to apply single pulse perturbations in state space beyond the manifold which separates the seizure and
259 non-seizure attractor (Suffczynski et al., 2004; Taylor et al., 2014b). While there is obvious appeal to
260 single pulse stimulation, there are many difficulties with that approach, especially in stochastic systems
261 where repeated success can be troublesome (Taylor et al., 2014b).

262 A second approach leverages methods from feedback control theory (Kramer et al., 2006; Ching et al.,
263 2012). While feedback control is the hallmark approach to deal with uncertainty, the controls developed
264 through optimal control provide several key advantages. In contrast, much of the work in neuroscience
265 using optimal control has dealt with stylized models that are analytically tractable (Li et al., 2013; Moehlis
266 et al., 2006). Such analytic results provide a unique level of intuition, however, are not scalable to general
267 large scale cases. We differentiate our work in this paper from the existing literature using control theory
268 for neuroscience applications in the following ways. Triggerred stimuli are applied on an “as needed”
269 basis (i.e. only when the SWD reaches a trigger point) in contrast to continuous feedback controllers
270 which are always on. From a patient perspective, this means that neurological function is identical to
271 pretreatment during the times between seizures. In contrast, feedback controllers continue to operate
272 and may as a consequence abate non-pathological neurological activity. While non-feedback methods
273 are often criticized for lack of robustness to noise and parameter uncertainties, recent development in
274 ensemble control allow robust open-loop controllers to be developed and demonstrated in past work with
275 the model used in this paper (Ruths et al., 2014; Ruths and Li, 2012). One limitation of optimal control
276 techniques is that they are highly dependent on the ability of the model to capture the clinically observed
277 EEG. While this is a limitation, models for neurological behavior are consistently improving, and the
278 method for control presented is highly general, so it can be applied to most models developed in the
279 future. The benefit gained from a known model is that the system is transferred reliably between the
280 states of interest (seizure state to background state). The underlying premise of optimal control is that
281 systems have moments in their dynamics when they are most and least susceptible to external influence.
282 The optimization process teases out these susceptible periods and designs the stimulus to take advantage
283 of them. Although feedback control can deliver a stimulus that adapts according to the state, it is typically
284 sub-optimal because it has no such information about susceptibility. Optimal control permits generating
285 stimuli that are minimal by design, so that the stimulus achieves the objective with the lowest, e.g., energy
286 or duration. Finally, the stimuli found through the optimal control process provide intuition on the nature
287 and dynamics of the of the system.

288 There are several benefits to the control strategy used here. First, only a subset of all variables are
289 controlled, in this case we only control the cortical variables PY and IN . In the experimental setting this
290 may be desirable because external noninvasive stimuli (e.g., transcranial magnetic stimulation) may not
291 fully penetrate to deep subcortical structures such as the thalamus. In our control of the spatially extended
292 model, the control is optimal in the sense that a cost function is optimized, given the consideration that
293 all cortical variables are available for control. This may be undesirable experimentally as a more spatially
294 localized solution may be sought, effectively reducing the number of locations that require stimulation to
295 abate the seizure. While such an optimal control problem is easy to formulate, solving this mixed-integer
296 problem is challenging on a problem of this size. An important direction of our future work will seek
297 to minimize the number of cortical areas stimulated through a variety of heuristic approaches. A further
298 benefit is that separate controls for each variable do not necessarily need to be developed for each variable.
299 We have demonstrated this throughout, where the same control has been applied to both the PY and IN

300 populations (see e.g. figure 4). Additionally, since the control profile is precomputed, the delivery of the
301 control could be applied in real-time when ‘trigger points’ on the SWD cycle are detected.

302 In this study, the same optimal controls are applied to both *PY* and *IN*, rather than developing different
303 controls for *PY* and for *IN*. In some experimental scenarios, it may be advantageous to differentiate
304 these neuron populations, for example, when using noninvasive stimuli such as TMS if the model does
305 not capture the variables controlled by the stimulus. In other applications this may not be necessary,
306 such as for invasive stimuli like optogenetics - where the specific variables are thought to be well known
307 (Selvaraj et al., 2014). Furthermore, the low dimensionality of SWD oscillations leads us to suggest
308 that only few variables may need to be controlled (Babloyantz and Destexhe, 1986). Nonetheless, the
309 method presented here is adaptable to generating either simultaneous or differentiated control signals for
310 the various neuron populations; this choice is driven based on the manner in which the stimulus interacts
311 with the tissue.

312 Interestingly the total strength of control required is different in different areas (figure 5d). Specifically
313 the lingual gyrus, which is important for vision, required high strength bilaterally. We hypothesize this
314 may be due to a hyperexcitability which may exist for photoparoxysmal response, which is common
315 in patients with IGE and absence epilepsy as is the patient studied here. We also find superior frontal
316 areas to require high stimulus strength. Indeed, superior frontal areas are heavily involved in spike-
317 wave seizures with many patients exhibiting frontally abnormal activity in EEG and functional MRI
318 recordings during seizures (Moeller et al., 2008; Bai et al., 2010). While many IGE patients do have
319 high amplitude abnormal frontal activity during seizures, abnormal activity in other areas is often more
320 patient-specific. This stereotypy is present in both the spatial and temporal aspects of the seizures in many
321 patients (Schindler et al., 2011). Indeed, as the seizure patterns exhibit stereotypy, even beyond SWD
322 seizures, so may the optimal control profiles.

323 One of the assumptions of our study is that the background state coexists with the SWD limit cycle in
324 the state space. This is essentially a different mechanistic assumption to that of a parameter change as in
325 some previous studies (Breakspear et al., 2006). In that case, control of the slowly varying parameter
326 can abate the seizure. In a recent study the modulation of a parameter was implemented as an ultra-slow
327 variable to cause seizure onset & offset (Jirsa et al., 2014). Indeed, our control strategy developed here
328 could easily be applied to such a slow variable as it would be incorporated as a state in an enlarged model.

329 We have incorporated clinical data into our model in the form of the connectivity, however, a next step
330 is to perform the control stimuli *in vivo*. This could be performed first in animal models of SWD (Meeren
331 et al., 2005), using high strength diffusion MRI to generate high resolution connectivity matrices (Besson
332 et al., 2014). Furthermore, with active perturbation it may be possible to elucidate the directionality of
333 connections (David et al., 2013), which would allow for the the application of network control theory
334 (Liu et al., 2011; Ruths and Ruths, 2014).

335 To summarize, we have demonstrated a nonlinear optimal control technique with application to epilepsy.
336 We have demonstrated its robustness in different settings, ultimately building up to a large scale model of
337 the brain which includes cortical connectivity derived from a patient with idiopathic generalized seizures.
338 We found that due to the heterogeneity in connectivity, there is heterogeneity in the optimal control
339 applied. We therefore suggest this should be considered when applying stimulation to large cortical areas
340 *in vivo* and that spatially localized solutions may consequently be more desirable.

DISCLOSURE/CONFLICT-OF-INTEREST STATEMENT

341 The authors declare that the research was conducted in the absence of any commercial or financial
342 relationships that could be construed as a potential conflict of interest.

343 The statement about the authors and contributors can be up to several sentences long, describing the
344 tasks of individual authors referred to by their initials and should be included at the end of the manuscript
345 before the References section.

ACKNOWLEDGMENTS

346 *Funding:* PNT and MK were supported by the Engineering and Physical Sciences Research Council
347 of the United Kingdom (EP/K026992/1) as part of the Human Green Brain Project (<http://www.greenbrainproject.org>). JT and JR were supported by the International Design Centre (Grant
348 IDG31300103). NS and JD were supported by the Ministry of Education (MOE) Tier 1 Grant M4011102
349 RGC3/13. PNT thanks Gerold Baier and Yujiang Wang for discussions regarding the model.
350

SUPPLEMENTAL DATA

351 Supplementary Material should be uploaded separately on submission, if there are Supplementary Figures,
352 please include the caption in the same file as the figure. LaTeX Supplementary Material templates can be
353 found in the Frontiers LaTeX folder

REFERENCES

- 354 Amari, S. (1977), Dynamics of pattern formation in lateral-inhibition type neural fields, *Biological*
355 *Cybernetics*, 27, 2, 77–87
- 356 Asconapé, J. and Penry, J. (1984), Some clinical and eeg aspects of benign juvenile myoclonic epilepsy,
357 *Epilepsia*, 25, 1, 108–114
- 358 Babajani-Feremi, A. and Soltanian-Zadeh, H. (2010), Multi-area neural mass modeling of EEG and MEG
359 signals, *NeuroImage*, 52, 3, 793–811
- 360 Babloyantz, A. and Destexhe, A. (1986), Low-dimensional chaos in an instance of epilepsy, *Proceedings*
361 *of the National Academy of Sciences*, 83, 10, 3513–3517
- 362 Bai, X., Vestal, M., Berman, R., Negishi, M., Spann, M., Vega, C., et al. (2010), Dynamic time course of
363 typical childhood absence seizures: EEG, behavior, and functional magnetic resonance imaging, *The*
364 *Journal of Neuroscience*, 30, 17, 5884
- 365 Baier, G., Goodfellow, M., Taylor, P., Wang, Y., and Garry, D. (2012), The importance of modelling
366 epileptic seizure dynamics as spatio-temporal patterns, *Frontiers in Physiology*, 3, 281
- 367 Berényi, A., Belluscio, M., Mao, D., and Buzsáki, G. (2012), Closed-loop control of epilepsy by
368 transcranial electrical stimulation, *Science*, 337, 6095, 735–737
- 369 Besson, P., Lopes, R., Leclerc, X., Derambure, P., and Tyvaert, L. (2014), Intra-subject reliability of the
370 high-resolution whole-brain structural connectome, *NeuroImage*, 102, 283–293
- 371 Blumenfeld, H. (2005), Cellular and network mechanisms of spike-wave seizures, *Epilepsia*, 46, 21–33
- 372 Blumenfeld, H. and Taylor, J. (2003), Why do seizures cause loss of consciousness?, *The Neuroscientist*,
373 9, 5, 301–310
- 374 Breakspear, M., Roberts, J., Terry, J., Rodrigues, S., Mahant, N., and Robinson, P. (2006), A unifying
375 explanation of primary generalized seizures through nonlinear brain modeling and bifurcation analysis,
376 *Cerebral Cortex*, 16, 9, 1296
- 377 Canuto, C., Hussaini, M., Quarteroni, A., and Zang, T. (2006), Spectral methods: Fundamentals in single
378 domains (Springer, Berlin)
- 379 Ching, S., Brown, E. N., and Kramer, M. A. (2012), Distributed control in a mean-field cortical network
380 model: implications for seizure suppression, *Physical Review E*, 86, 2, 021920

- 381 Conte, A., Gilio, F., Iacovelli, E., Bettolo, C., Di Bonaventura, C., Frasca, V., et al. (2007), Effects of
382 repetitive transcranial magnetic stimulation on spike-and-wave discharges, *Neuroscience Research*, 57,
383 1, 140–142
- 384 David, O., Job, A.-S., De Palma, L., Hoffmann, D., Minotti, L., and Kahane, P. (2013), Probabilistic
385 functional tractography of the human cortex, *Neuroimage*, 80, 307–317
- 386 Deco, G., Ponce-Alvarez, A., Mantini, D., Romani, G. L., Hagmann, P., and Corbetta, M. (2013), Resting-
387 state functional connectivity emerges from structurally and dynamically shaped slow linear fluctuations,
388 *The Journal of Neuroscience*, 33, 27, 11239–11252
- 389 Desikan, R. S., Ségonne, F., Fischl, B., Quinn, B. T., Dickerson, B. C., Blacker, D., et al. (2006), An
390 automated labeling system for subdividing the human cerebral cortex on mri scans into gyral based
391 regions of interest, *Neuroimage*, 31, 3, 968–980
- 392 Destexhe, A. (1998), Spike-and-wave oscillations based on the properties of GABAB receptors, *The*
393 *Journal of Neuroscience*, 18, 21, 9099
- 394 Fornberg, B. (1998), A practical guide to pseudospectral methods, volume 1 (Cambridge university press)
- 395 Haimovici, A., Tagliazucchi, E., Balenzuela, P., and Chialvo, D. R. (2013), Brain organization into resting
396 state networks emerges at criticality on a model of the human connectome, *Physical review letters*, 110,
397 17, 178101
- 398 Honey, C., Sporns, O., Cammoun, L., Gigandet, X., Thiran, J.-P., Meuli, R., et al. (2009), Predicting
399 human resting-state functional connectivity from structural connectivity, *Proceedings of the National*
400 *Academy of Sciences*, 106, 6, 2035–2040
- 401 Jirsa, V. K., Stacey, W. C., Quilichini, P. P., Ivanov, A. I., and Bernard, C. (2014), On the nature of seizure
402 dynamics, *Brain*, 137, 8, 2210–2230
- 403 Kalitzin, S., Velis, D., and Lopes da Silva, F. (2010), Stimulation-based anticipation and control of state
404 transitions in the epileptic brain, *Epilepsy & Behavior*, 17, 3, 310–323
- 405 Keränen, T., Sillanpää, M., and Riekkinen, P. J. (1988), Distribution of seizure types in an epileptic
406 population, *Epilepsia*, 29, 1, 1–7
- 407 Kramer, M. A. and Cash, S. S. (2012), Epilepsy as a disorder of cortical network organization, *The*
408 *Neuroscientist*, 18, 4, 360–372
- 409 Kramer, M. A., Lopour, B. A., Kirsch, H. E., and Szeri, A. J. (2006), Bifurcation control of a seizing
410 human cortex, *Physical Review E*, 73, 4, 041928
- 411 Li, J.-S., Dasanayake, I., and Ruths, J. (2013), Control and Synchronization of Neuron Ensembles, *IEEE*
412 *Transactions on Automatic Control*, 58, 8, 1919–1930
- 413 Liang, S.-F., Shaw, F.-Z., Chang, D.-W., Young, C.-P., Wang, Y. L., and Wu, S. Y. (2012), Live
414 demonstration: A portable closed-loop seizure controller in freely moving rats, in Biomedical Circuits
415 and Systems Conference (BioCAS), 2012 IEEE (IEEE), 88–88
- 416 Liang, S.-F., Shaw, F.-Z., Young, C.-P., Chang, D.-W., and Liao, Y.-C. (2010), A closed-loop brain
417 computer interface for real-time seizure detection and control, in Engineering in Medicine and Biology
418 Society (EMBC), 2010 Annual International Conference of the IEEE (IEEE), 4950–4953
- 419 Liu, Y., Slotine, J., and Barabási, A. (2011), Controllability of complex networks, *Nature*, 473, 7346,
420 167–173
- 421 Luenberger, D. G. (1968), Optimization by vector space methods (John Wiley & Sons)
- 422 Marten, F., Rodrigues, S., Suffczynski, P., Richardson, M., and Terry, J. (2009), Derivation and analysis of
423 an ordinary differential equation mean-field model for studying clinically recorded epilepsy dynamics,
424 *Physical Review E*, 79, 2, 021911
- 425 Meeren, H., van Luijckelaar, G., Lopes da Silva, F., and Coenen, A. (2005), Evolving concepts on the
426 pathophysiology of absence seizures: the cortical focus theory, *Archives of neurology*, 62, 3, 371
- 427 Messé, A., Rudrauf, D., Benali, H., and Marrelec, G. (2014), Relating structure and function in the
428 human brain: relative contributions of anatomy, stationary dynamics, and non-stationarities, *PLoS*
429 *computational biology*, 10, 3, e1003530
- 430 Moehlis, J., Shea-Brown, E., and Rabitz, H. (2006), Optimal inputs for phase models of spiking neurons,
431 *Journal of Computational and Nonlinear Dynamics*, 1, 358
- 432 Moeller, F., Siebner, H., Wolff, S., Muhle, H., Granert, O., Jansen, O., et al. (2008), Simultaneous
433 EEG-fMRI in drug-naive children with newly diagnosed absence epilepsy, *Epilepsia*, 49, 9, 1510–1519

- 434 Pinault, D. and O'Brien, T. (2005), Cellular and network mechanisms of genetically-determined absence
435 seizures, *Thalamus & Related Systems*, 3, 3, 181
- 436 Rajna, P. and Lona, C. (1989), Sensory stimulation for inhibition of epileptic seizures, *Epilepsia*, 30, 2,
437 168–174
- 438 Robinson, P. A., Rennie, C. J., and Rowe, D. L. (2002), Dynamics of large-scale brain activity in normal
439 arousal states and epileptic seizures, *Physical Review E*, 65, 4, 041924
- 440 Ruths, J. and Li, J.-S. (2012), Optimal Control of Inhomogeneous Ensembles, *Automatic Control, IEEE*
441 *Transactions on*, 57, 8, 2021–2032
- 442 Ruths, J. and Ruths, D. (2014), Control Profiles of Complex Networks, *Science*, 343, 6177
- 443 Ruths, J., Taylor, P., and Dauwels, J. (2014), Optimal control of an epileptic neural population model, in
444 International Federation of Automatic Control World Congress, volume 19, volume 19, 3116–3121
- 445 Sadleir, L., Farrell, K., Smith, S., Connolly, M., and Scheffer, I. (2006), Electroclinical features of absence
446 seizures in childhood absence epilepsy, *Neurology*, 67, 3, 413–418
- 447 SAILLET, S., Gharbi, S., Charvet, G., Deransart, C., Guillemaud, R., Depaulis, A., et al. (2012), Neural
448 adaptation to responsive stimulation: A comparison of auditory and deep brain stimulation in a rat
449 model of absence epilepsy, *Brain Stimulation*
- 450 Schindler, K., Gast, H., Stieglitz, L., Stibal, A., Hauf, M., Wiest, R., et al. (2011), Forbidden ordinal
451 patterns of periictal intracranial EEG indicate deterministic dynamics in human epileptic seizures,
452 *Epilepsia*
- 453 Selvaraj, P., Sleight, J. W., Freeman, W. J., Kirsch, H. E., and Szeri, A. J. (2014), Open loop optogenetic
454 control of simulated cortical epileptiform activity, *Journal of computational neuroscience*, 36, 3, 515–
455 525
- 456 Sporns, O., Tononi, G., and Kötter, R. (2005), The human connectome: a structural description of the
457 human brain, *PLoS computational biology*, 1, 4, e42
- 458 Suffczynski, P., Kalitzin, S., and Lopes Da Silva, F. (2004), Dynamics of non-convulsive epileptic
459 phenomena modeled by a bistable neuronal network, *Neuroscience*, 126, 2, 467–484
- 460 Takens, F. (1981), Detecting strange attractors in turbulence, in *Dynamical systems and turbulence*,
461 Warwick 1980 (Springer), 366–381
- 462 Taylor, P. and Baier, G. (2011), A spatially extended model for macroscopic spike-wave discharges,
463 *Journal of Computational Neuroscience*, 31, 3, 679–684
- 464 Taylor, P. N., Baier, G., Cash, S. S., Dauwels, J., Slotine, J.-J., and Wang, Y. (2013a), A model of stimulus
465 induced epileptic spike-wave discharges, *IEEE Symposium Series on Computational Intelligence*, 53–
466 59
- 467 Taylor, P. N., Goodfellow, M., Wang, Y., and Baier, G. (2013b), Towards a large-scale model of patient-
468 specific epileptic spike-wave discharges, *Biological cybernetics*, 107, 1, 83–94
- 469 Taylor, P. N., Kaiser, M., and Dauwels, J. (2014a), Structural connectivity based whole brain modelling
470 in epilepsy, *Journal of neuroscience methods*
- 471 Taylor, P. N., Wang, Y., Goodfellow, M., Dauwels, J., Moeller, F., Stephani, U., et al. (2014b), A
472 computational study of stimulus driven epileptic seizure abatement, *PloS one*, 9, 12, e114316
- 473 Terry, J. R., Benjamin, O., and Richardson, M. P. (2012), Seizure generation: The role of nodes and
474 networks, *Epilepsia*, 53, 9, e166–e169
- 475 Wang, Y., Goodfellow, M., Taylor, P., and Baier, G. (2012), Phase space approach for modeling of
476 epileptic dynamics, *Physical Review E*, 85, 6, 061918
- 477 Westmijse, I., Ossenblok, P., Gunning, B., and Van Luijtelaar, G. (2009), Onset and propagation of spike
478 and slow wave discharges in human absence epilepsy: a MEG study, *Epilepsia*, 50, 12, 2538–2548
- 479 Yan, B. and Li, P. (2013), The emergence of abnormal hypersynchronization in the anatomical structural
480 network of human brain, *Neuroimage*, 65, 34–51
- 481 Yeh, F.-C., Wedeen, V. J., and Tseng, W.-Y. (2010), Generalized-sampling imaging, *Medical Imaging*,
482 *IEEE Transactions on*, 29, 9, 1626–1635

FIGURES

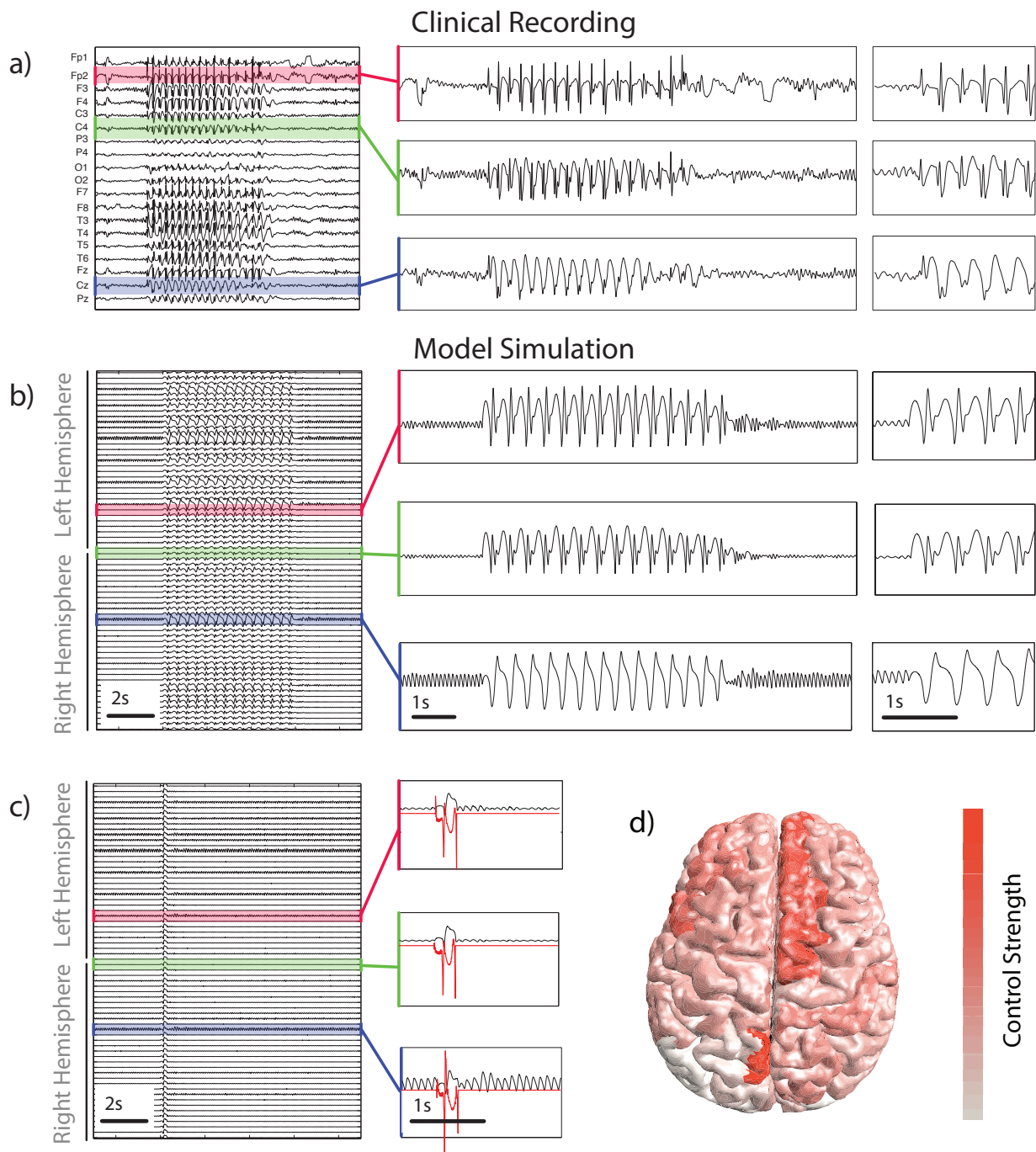


Figure 5. Control derived using patient-specific connectivity a) Clinical EEG recording of a SWD seizure from 19 scalp electrodes. b) and c) show time series of simulated activity without and with the control switched on. Without the control the simulated seizure lasts several seconds. Control is shown in red in c) in three inset panels. c) Spatial distribution of the total strength required to control the seizure. Warmer colors indicate a greater strength is applied in those areas.